

MSc Thesis

Forecasting the glacial landscapes in Altai mountains based on modelling

Cold Region Environmental Landscapes Integrated Sciences

CORELIS

BORBÁLA FARKAS



St Petersburg
University



Scientific supervisor:

Reviewer:

PROF. DR. DMITRY A. GANYUSHKIN ASS. PROF. DR. OLEG V. OSTANIN

Institute of Earth Sciences

Saint Petersburg State University

Saint Petersburg, Russia

6 June 2022

CORELIS

Master Thesis

2022

**Forecasting the glacial landscapes in Altai
mountains based on modelling**

Scientific supervisor:

PROF. DR. DMITRY A. GANYUSHKIN

Saint Petersburg State University

Saint Petersburg, Russia

Reviewer:

ASS. PROF. DR. OLEG V. OSTANIN

Altai State University

Barnaul, Russia

Contents

1	Introduction	1
1.1	Geographical and Climatological Setting	2
1.2	Previous work	5
1.3	Snowline, Equilibrium Line Altitude and Accumulation Area Ratio	7
2	Materials and methods	9
2.1	Remote sensing	10
2.1.1	Uncertainties of remote sensing	11
2.2	Weather stations	12
2.3	Kurowski method	14
2.4	ELA determination	15
2.5	AAR determination	16
3	Results	17
3.1	Temperature and precipitation	17
3.2	Equilibrium line altitude	20
3.3	Accumulation area ratio	25
4	Discussion	29
4.1	Tendencies in the temperature and precipitation	29
4.2	Forecasting the glacial behavior	30
5	Conclusion	33

Abstract

Tavan Bogd massif is very poorly studied, although it is the largest glacierized area in the Altai mountains. In this master thesis, 10 larger valley glaciers of Tavan Bogd were examined in the last three decades from 1989 to 2020. The purpose of this work was to find the general trend in the recent changes of Tavan Bogd glaciers and use it to predict the future behavior of these larger glaciers. The main focus was to find correlation between the properties of glaciers and the climate variables. Using satellite pictures, the equilibrium line altitude (ELA) of each glacier were determined for 8 years (1989, 2000, 2010, 2016, 2017, 2018, 2019, 2020). The temperature and precipitation data were obtained from the closest, Kosh-Agach meteorological station. Based on the calculations, a strong relation was found between the temperature and the ELA. The general trend is that $1^{\circ}C$ temperature change results $66.5m$ change in the ELA. However, precipitation did not show correlation. Calculations for the accumulation area ratio (AAR) was also made and the typical AAR was declared at $AAR_{avg} = 0.563$. Using the developed method, modelling the glacial behavior was successful and it became possible to give predictions for the future properties of glaciers, such as glacial termini or area, in the Tavan Bogd massif.

1 Introduction

Glaciers are large masses of perennial ice moving slowly downwards on a slope. They are made from the fallen, then recrystallised snow throughout the years. During glacier formation, snow remains in one location for enough time to be compressed into ice. Due to their constant flow, they can be considered as very slow rivers of ice, which made them unique.

During the Pleistocene Epoch (lasted from about 2,6 million to 11700 years ago), which includes Last Glacial Maximum[1] (LGM) about 20000 years ago, glacial extension was almost 30 percent of the world's land area, but in other interglacial periods, the glacial coverage dropped under its present extent. After the LGM, a huge glacial retreat started, which also resulted a global sea level rise about 125 meters[2], compared to today's sea level. Currently, glaciers occupy about the 11 percent of total land area of the world[3], including ice caps and ice sheets. They are located mostly in polar regions like Antarctica or Canadian Arctic, but can be found in all parts of the world, even at almost all latitudes, for instance in Uganda.

Glacial formation happens, when the accumulation period of snow exceeds the ablation period. It strongly depends on precipitation and temperature and takes many steps while the deposited snow transforms and recrystallises into ice. Usually, the formation lasts more than a hundred year and each year a new layers of snow buries and gets compressed into ice. Therefore, the density of a glacier increases with the depth, it can reach more than 900 kilograms per cubic metres[4].

However, glaciers are very vulnerable for climate change, especially

mountain glaciers, hence, they could be natural indicators of climate. The smaller the glaciers are, the more sensible they are, so small mountain glaciers react firstly to the climate changes. From the end of the 19th century, a worldwide glacial retreat was observed after the LIA (Little Ice Age) maximum. From the 20th century this retreat can be modelled with a linear trend which corresponds to the temperature increase of $+0.66^{\circ}C$ per century[5]. Since glaciers are significant source of water, the annual ice loss causes a huge problem in the surrounding areas. The meltwater can also cause rise in the sea level, which is critical for the coastal flooding [6] and might cause huge problems in the future.

The aim of my work, to find a correlation between recent behavior of Tavan Bogd glaciers and the changes of climate variables. In my work, I studied the dynamics of the larger glaciers of Tavan Bogd. First, I analyzed the recent changes of properties such as equilibrium line altitude and accumulation area ratio in accordance to the temperature and precipitation changes measured by weather station near to the examined area. I used satellite pictures for each year and processed them with geographic information system services. I also used data from previous researches to supplement my results, on one hand, to get a wider timeline and picture, on the other hand, to compare my calculation with previous results. Based on that information, it might become possible to find a trend in glacial behavior and predict the future state of the glaciers.

1.1 Geographical and Climatological Setting

The study area of this master thesis is the glaciers of the Tavan Bogd massif, which is situated in the Altai mountain region. The Altai moun-

tain ridge is found in the south of Siberia and in Central Asia, on the border of four countries (Russian Federation, Mongolia, Kazakhstan and China) and can be divided into the Russian Altai and the Mongolian Altai. It includes long mountain ridges like Shapshalsky, Tsagan-Shibetu, Chikhacheva or Saylugem in the Russian Altai and separated mountain masses in the Mongolian Altai. The whole area covers approximately $90\,000\text{km}^2$ and the Tavan Bogd massif spreads out in 2600km^2 . This massif is poorly studied, although it is the largest glacierized area of Altai. The elevation sometimes exceeds 4000m a.s.l. (Tsambagarav). The highest peak, situated in Mongolia, is Khuiten Uul with the elevation 4374m a.s.l. In Figure 1., the situation of Tavan Bogd can be seen.

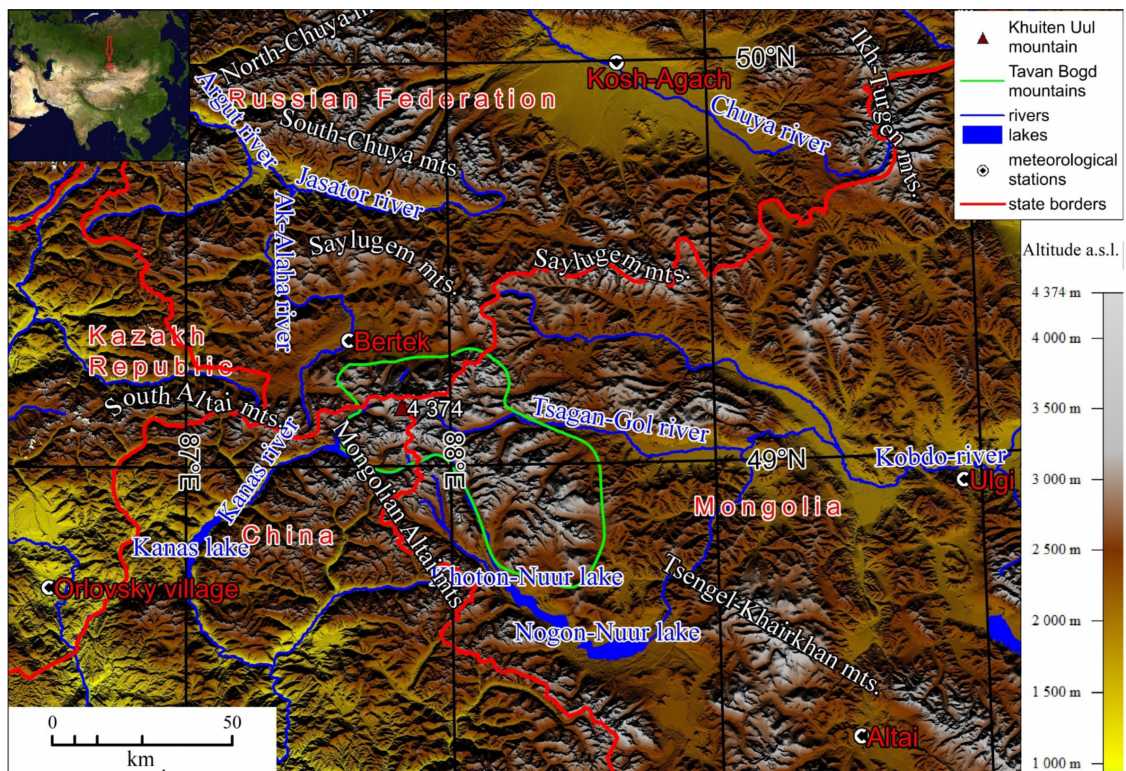


Figure 1: Geographical location of Tavan Bogd massif in the Altai region[7].

In the massif, the number of total glaciers is 243 and their area covers 353.4km^2 [7]. There are mostly large valley glaciers, but hanging and cirque glaciers are also significant. Glacier relief forms can also be found in this area such as moraines and U-shaped valleys.

The climate of the area is poorly studied, mostly because meteorological stations are rare and far away from the glaciers. In addition, most of them are situated more than $1km$ lower than the studied glacial area. The meteorological data for the northern slopes are better known, because there was a weather station (Bertek) functioned between 1959 and 1982. It was only $10km$ away from the glaciers and on the altitude $2250m$ a.s.l. After it was close, we could only rely data from further meteorological station, hence, current data is less accurate.

However, climatic conditions are mostly cold and arid with negative annual mean temperature, which is around $-3^{\circ}C$. The annual average precipitation at the north-eastern foot of the massif is very low, about $160mm$ and it comes mostly from northern (Argut river valley and Katun river valley) and western (ultimate western part of the Tavan Bogd massif) direction. Most percent of the precipitation falls in the summer period (around 59%) and there are almost no snow in winters (around 5%)[8]. It can be explained with the effect of the Asian anticyclone in the arid winter and the south-western cyclones (from the Aral, Caspian and, to a lesser extent, Black Seas) in the summer and autumn, when most of the snowfall happens. The western southwestern part of the massif is opened through the valley of the Bukhtarma River and Kanas river and climatic conditions are less known because of the distance of weather stations.

Nowadays, the closest weather station is located in Kosh-Agach ($1759m$ a.s.l.), about $100km$ from the glaciers of Tavan Bogd in the northeastern direction. From the eastern side, the closest is Ulgi station ($1715m$ a.s.l.) with the distance of $150km$ and from the south-west Kazakhstan-

Orlovskiy (1106m a.s.l.), which is 90km away from Tavan Bogd. In the west direction, there are also Katon-Karagai (1081m a.s.l.), about 140km. In China, the nearest weather stations are Altai (2182m a.s.l.) about 140km to the east.

Based on the data from these stations a general increase can be observed in temperature from the northwest to the southeast. Precipitation also has a large difference between the western and eastern part of the massif it decreases towards to southeast from more than 1000mm to less than 400mm. These two conditions lead to the general rising of the equilibrium line altitude about 500m from the northwest to the southeast[9].

Also, in the past decades a warming was observed in the region, for example in Kosh-Agach station the mean summer temperature has risen about 1.5°C in ten years between the 1990s and the 2000s, which results huge degradation in glacial area and mass. Despite of the fact that the decline is slowed down after 2009, the retreat of glacial area was approximately 0.9%/year in the northern slope of Tavan Bogd. Small glaciers were better expose to the warming and degraded more than the larger glaciers.

1.2 Previous work

Glaciers in the Tavan Bogd massif were first described by a Russian researcher, V.V. Sapozhnikov in 1897[10]. He discovered the largest glacier in Tavan Bogd, the Potanin Glacier. From 1905 to 1909, he mapped all the main glaciers of the massif. In 1925, "Catalog of Altai Glaciers" was published by B.V. Tronov[11]. He described the Tavan

Bogd massif with 36 glaciers and a total area of $158km^2$.

The next research happened in 1959, when Chinese researchers studied the southern part of the Tavan Bogd glacier system and as a result, this area is in the “Glacier Inventory of China”[12]. The next expansion was the “Catalog of Glaciers of the USSR” (UGI), which was published in the period of 1965–1982[13]. In the Mongolian part of Tavan Bogd, the snow-firn area of glaciers, estimated by aerial photographs, was $94km^2$ in the year of 1971[14]. The total area of Tavan Bogd was estimated by a Soviet-Mongolian glaciological expedition in 1987 and gave the result of $222.3km^2$ [15].

From the year of 1999, the northern slopes of the massif are repeatedly studied by the researchers of Saint Petersburg State University using both remote sensing and in situ observations[8]. Due to the development of the remote sensing methods, a huge improvement occurred in the studies of Tavan Bogd, which resulted that the Mongolian part of the massif was estimated the area of $95.2km^2$ [16], while as a outcome of the “Second Chinese Glacier Inventory”, the estimated area of the Chinese part of the massif was $76km^2$ [17]. Beside that, according to the Global Land Ice Measurements from Space (GLIMS) database and the Randolph Glacier Inventory, the result about the total area of glacialization is $204km^2$ [18]. In spite of the results above, there are still unknown conditions regarding the climate variables and glacial properties in the studied region.

1.3 Snowline, Equilibrium Line Altitude and Accumulation Area Ratio

The equilibrium line altitude (ELA) separates the accumulation area and ablation area on a glacier. By definition, it is a theoretical altitude, where the ablation and accumulation rate of a glacier are equal to each other over a 1-year period. It can be described as the altitude, where the net mass balance equals zero[19].

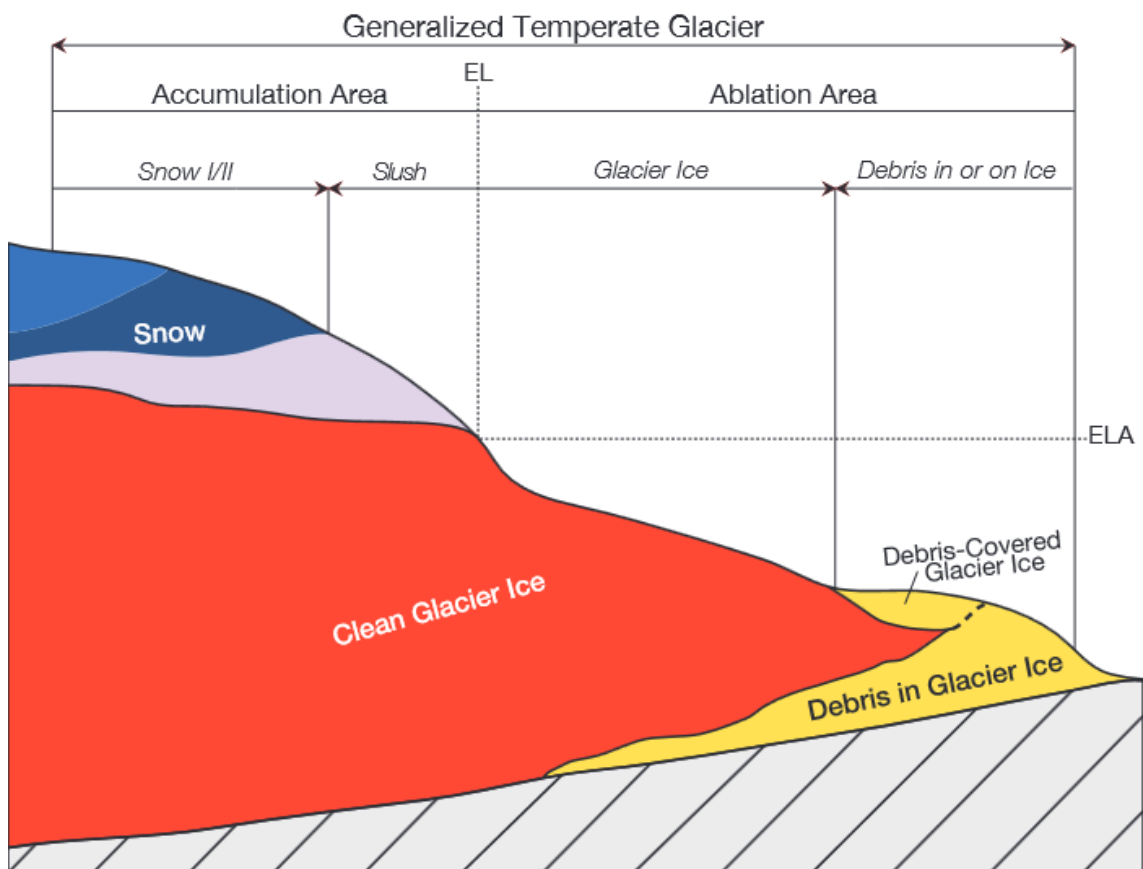


Figure 2: Generalized temperate glacier showing ELA and the classified glacier facies. Wet Snow = Dark Blue, Snow = Light Blue, Slush = Grey, Ice = Red, Debris in or on Ice = Yellow[20].

In practice, it means that if the accumulation area increases (or other way, the ablation area decreases) the equilibrium line will get closer to the margin of the glaciers and has a lower altitudinal position.

In the Altai mountain ridge, because of the special climate conditions, the winters are arid, so the ablation period overlaps with the hu-

mid months and as a consequence, most of the snow fall in the autumn months, when there is still chance for precipitation, but the temperature already became cold enough. Therefore in the end of the ablation period, there is a short interval, when snow melts and the lower snow boundary (snowline) reaches its maximum altitude. It marks approximately the equilibrium line altitude[21]. In this master thesis, from all these considerations above, I used satellite images taken from the end of the ablation season.

After defining the ELA, the accumulation area and the ablation area can be calculated. The ratio of the accumulation area compared to the whole area of a glacier is called the accumulation-area ratio (AAR)[22].

$$AAR = \frac{A_{acc}}{A_{acc} + A_{abl}} \quad (1)$$

where the A_{acc} and A_{abl} sign the area of accumulation and ablation, respectively. Usually, this ratio is between 0.5 and 0.8 for glaciers which are in in climatic-geometric balance and situated in higher altitudes, but lower for glaciers which are degrading[23]. In this work, I process the satellite pictures with Geographical Information Systems (GIS) using Digital Elevation Models (DEM) to get the equilibrium line altitude.

2 Materials and methods

This thesis is based on continuous remote sensing monitoring and meteorological data collected from the past decades. During my work, I obtained satellite images approximately from the past 30 years and I analyzed them to acquire the ELA. I used images from the years 2016, 2017, 2018, 2019 and earlier results of ELA from the years 1989, 2000, 2010, 2020[24]. The reason of choosing the analyzed years was that after 2015, Sentinel-2 images are available with much higher resolution compared to the imagery of Landsat satellites and other widely used imagery techniques in the past.

I also use the temperature and precipitation data[25], which can be obtained for every month of the year for the period I studied (between 1989-2020). The series of these climate variables can give a comparison to see the changes in the ELA and predict the future glacial dynamics.

The examined glaciers are mostly larger valley glaciers, which gives us the opportunity to study a longer time period. They are less vulnerable to rapid changes in climate variables, then other type of glaciers like hanging glaciers, which are usually also smaller and very dependent on precipitation or slope angle. Moreover, larger glaciers usually have a more distinct, sharper margin that is easier to mark on satellite imagery. Consequently, the tendencies in their dynamics can be obtained better, which makes them more suitable to consider them as a climate indicator and use them as an object in this work.

2.1 Remote sensing

Remote sensing is widely used method, to observe glacial landscapes, especially in the current century, where the extracted images have much more better resolution. This method gives the opportunity to observe the current state of the glaciers, even day by day frequency.

All used satellite picture were provided by the United States Geological Survey (USGS)[26], but they can be classified based on their resolution. The reason for the different resolutions that, in the past, only lower resolution images were available.

Image ID	Date	Spacecraft	Spatial resolution [m]
LT41430261989246XXX02	3 September 1989	Landsat 4	30
LE71440262000220SGS00	7 August 2000	Landsat 7	15
LE71430262000229SGS00	16 August 2000	Landsat 7	15
SP5_214251_100831	31 August 2010	SPOT 5	2.5
S2A_OPER_MSI_L1C_TL_MTI	30 August 2016	Sentinel-2A	10
L1C_T45UWQ_A010927	26 July 2017	Sentinel-2A	10
L1C_T45UWQ_A007624	22 August 2018	Sentinel-2B	10
L1C_T45UWQ_A007338	2 August 2018	Sentinel-2B	10
L1C_T45UWQ_A021609	12 August 2019	Sentinel-2A	10
L1C_T45UWQ_A026471	17 July 2020	Sentinel-2A	10

Table 1: Satellite images of Tavan Bogd with their resolution

In Table 1. the satellite images I used can be seen. Most of them are represented by Sentinel-2 imagery, which can be regarded having a high resolution, with the maximal spatial resolution of 10m. After acquiring the appropriate images, the combination of color band $B04$, $B03$, $B02$ was used, which gives a True-Colour Image as an RGB (red, green, blue) channel. It greatly facilitates to distinguish seasonal snow

to the firn line, also makes it easier to delimit moraines or the spatial distribution of glaciers. Moreover, in the case of Sentinel images, all of these three color bands have the same spatial resolution ($10m$), so the combination of bands did not reduce the resolution of the final picture, used in this master thesis.

These images should have gone through numerous requirements and were chosen according to many factor. First, the date should have been very close to the end of the ablation season, finding the highest snow line, which gives us the best estimation during the delineation of the ELA. Second, the percentage of the cloud cover should have been low enough that the glaciers could be visible. Third, also, it was important to avoid satellite images after snowfall, because it interferes the contours of the glaciers and can result misleading delineation.

2.1.1 Uncertainties of remote sensing

There are several uncertainties, which can cause possible mistakes at many point of the calculations. They can be divided into two types, systematic errors and random errors. The systematic errors came from the satellite imagery, which has an uncertainty of ± 1 pixel. The resolution of the imagery is $10m$, hence the drew equilibrium line during delineation process has the uncertainty of $10m$. The appearing systematic error while calculating the area can be described with the following formula:

$$A^{error} = n \cdot m \quad (2)$$

Where n marks the number of pixels forming the perimeter of the area of the glacier and m marks the area of one pixel with the spatial resolution of the picture.

However, there are several error opportunities during the process of delineation. Both the equilibrium lines and the contours of the glaciers were made manually, which can lead some random errors. There were two main error factors during manual delineation.

First, it is easy to draw the equilibrium line in a wrong position (usually closer the margin of the glacier) if the picture was taken after snowfalls or not exactly the end of the melting season. To avoid it, photos was chosen from the end of the ablation season, although sometimes it was hard to find the proper picture. For some glacier, I had to use more than one picture to get the most appropriate result, but in some cases it still did not give the perfect result. The other similar problem is snow patches. They can be also confusing, especially in the case of smaller glaciers, which makes hard to distinguish the area or mark the equilibrium line. Finding definite edges or some glacial structure might help to isolates glaciers from snow patches.

Second, cloud cover can be also a problem. Sometimes, when the equilibrium line is clearly visible for one glacier, others are covered by clouds. It can be resolved with also using pictures taken at different time. For example, that was the reason why two images were used, in the year 2018, seen in Table 1. Choosing different pictures can also help avoiding the cases when some part of the glacier are shaded and delineation became very inaccurate.

2.2 Weather stations

The temperature and precipitation data came from the *Kosh-Agach* weather station[25], which is located in the north east direction to the

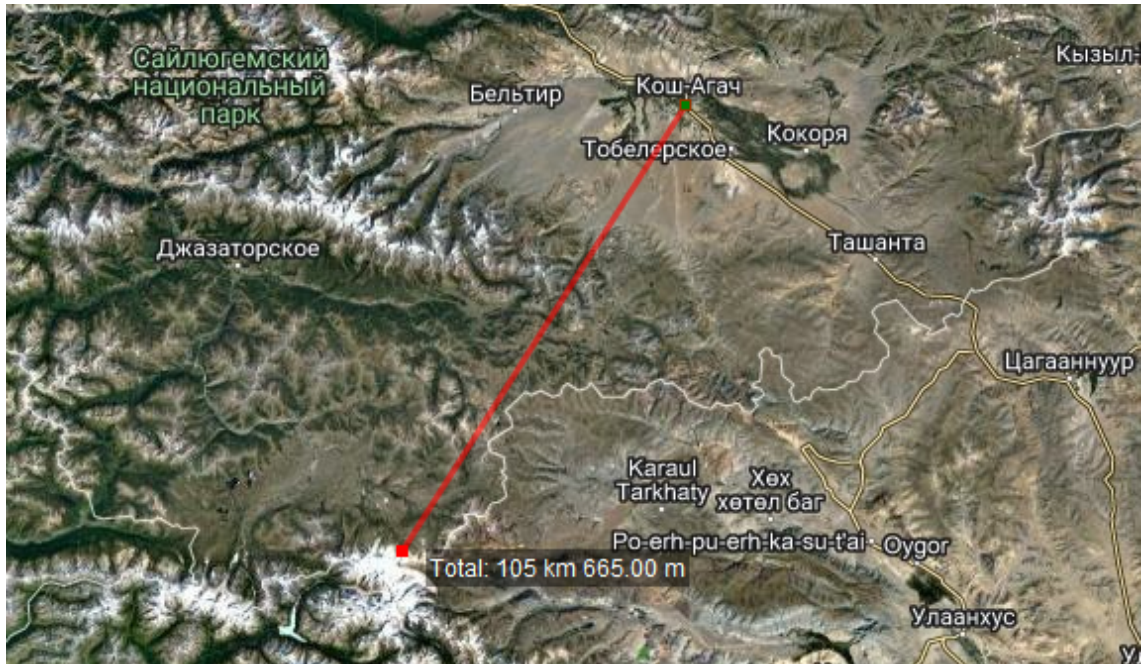


Figure 3: The distance of the Kosh-Agach meteorological station from the Tavan Bogd massif. Picture was made with SAS.Planet¹.

Tavan Bogd massif. It is approximately 100km away from the northern slopes of the glaciers at north latitude $50^{\circ}00'$ and east longitude $88^{\circ}40'$ in the altitude of 1759m a.s.l. This is one of the closest meteorological station which provides data after Bertek station was closed in 1982. In Figure 3. the location of Kosh-Agach and its distance from Tavan Bogd are seen. It was found that the temperature data from Bertek is highly correlates with the temperature of data from Kosh-Agach[27]. Unfortunately, the precipitation data does not show much correlation between the two station. The reason is that, the prevailing precipitation comes from the west and because of the varying relief from the west to the east, it can change much in a short distance or in different altitudes. The data from the weather station was processed with the package pandas 1.4.2[28] in Python 3.10.4[29] language. Figure 4. shows the changes in temperature and precipitation over the years.

¹<http://www.sasgis.org/sasplaneta/>

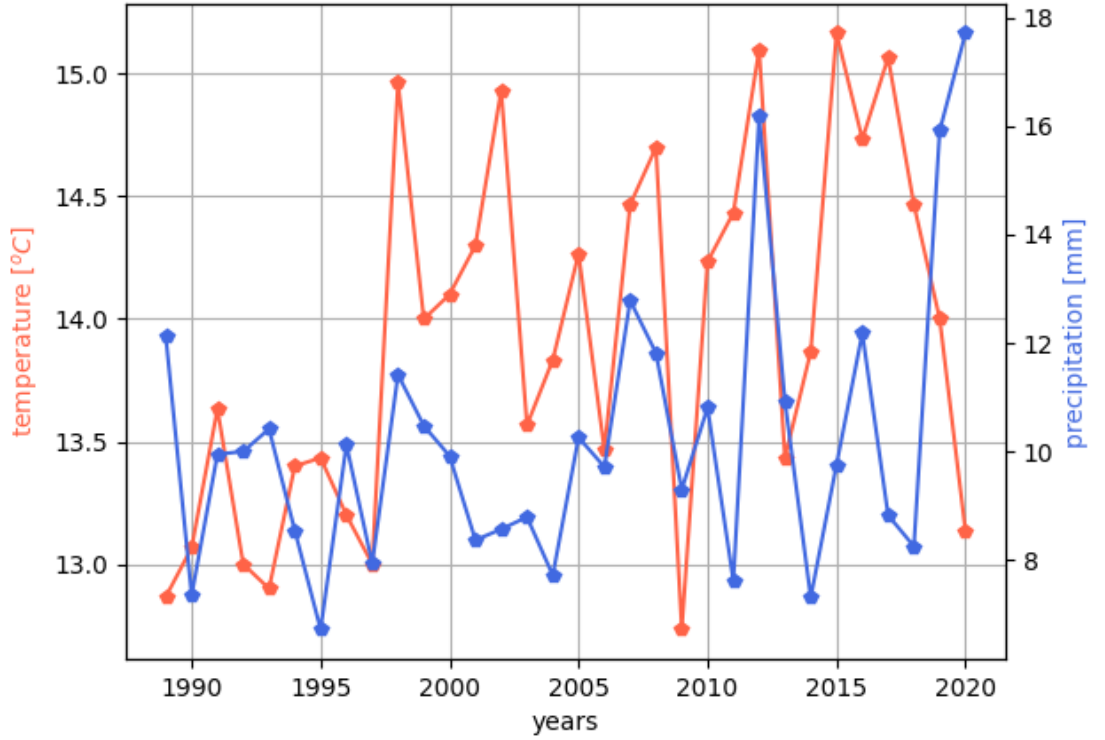


Figure 4: Average summer temperature and average annual precipitation data from Kosh-Agach meteorological station between 1989 and 2020.

2.3 Kurowski method

Lugwig Kurowski (born is 1866) proposed a new method for determining the ELA[30]. His idea is based on the assumption that the vertical gradient of mass balance is constant through the whole altitude interval of the glacier.

$$\left(\frac{db}{dh}\right)_{glacier} = const. \quad (3)$$

Where b signs the specific mass balance and h is the height. If this condition is satisfied and the accumulation is in balance with the melting, the snow line altitude (which is the equilibrium line altitude in this case) is equal to the mean altitude of the glacier. Hence, with the Kurowski

method, ELA could be calculated by the following formula:

$$ELA = \frac{\sum_{i=1}^{i=N} h_i \cdot a_i}{\sum_{i=1}^{i=N} a_i} \quad (4)$$

Here, the glacier was divided into altitude bands and for every band, the area of the specific band (a_i) is multiplied with the height of the band (h_i). The sum of the product is divided with the total area of the glacier $A = \sum_{i=1}^{i=N} a_i$.

However, this method was often misunderstood in the past and was confused with the median altitude[31], which is the altitude of the line, which splits the area of the glacier into two equal halves.

It was found that, Kurowski's assumption concerning the gradient of mass balance is not exactly correct[32]. Glaciers can be described with a term, named balance ratio, which gives a more precise description.

$$BR = \frac{\left(\frac{db}{dh}\right)_{abl}}{\left(\frac{db}{dh}\right)_{acc}} \quad (5)$$

If the balance ratio is bigger than 1, the ELA will shift and the increased BR will result a lower theoretical ELA[33].

As a conclusion, Kurowski's theoretical ELA can be used to verify the calculated ELA based on satellite images and remote sensing.

2.4 ELA determination

After choosing the most accurate Sentinel-2 pictures from United States Geological Survey[26], I processed them with ArcGIS 10.4.1[34], which

is a geographic information system services developed and maintained by Esri. To get natural color pictures, I combined the three RGB channels ($B04$, $B03$, $B02$) with raster processing. Then, I used `Global mapper v21.1`² to delineate the snowline for each glaciers using line feature tool. After delineation, to calculate the ELA, I used an SRTM digitam elevation model[35] (DEM) which has the resolution of 1 arc-second (or $30m$). The calculations were made automatically in `Global Mapper` using Digitizer Tool and characterized many properties of the glacier, included the average elevation, what can be used as the equilibrium line altitude. Due to the limited resolution of the DEM, it also carries the possibilities of some systematic errors in the ELA.

2.5 AAR determination

Accumulation area ratio calculation has also been done for the studied galciars. To perform it, the delineations of the equilibrium line and the contours of the glaciers were used. The contours were taken from the year 2010, and since the area of glaciers are not changing significantly over the years, the same contour could be used for every examined year. The calculation was done in `MapInfo Pro 15.0`[36] creating the accumulation area from the equilibrium line and contours. The area was determined automatically by the program.

²<https://www.bluemarblegeo.com/global-mapper/>

3 Results

I examined 10 larger glaciers in the study area of Tavan Bogd. I processed the satellite pictures, delineate the snow line and calculated the the equilibrium line altitude for four consecutive years (2016, 2017, 2018, 2019) and the year 1989. In Figure 5., the contours of each glaciers are shown. The contour was made for the year 2010[24], which is the closest available contour in time. It can be used for all the years with a good approximation, because the change in the contours of the glaciers is negligible during the examined period.

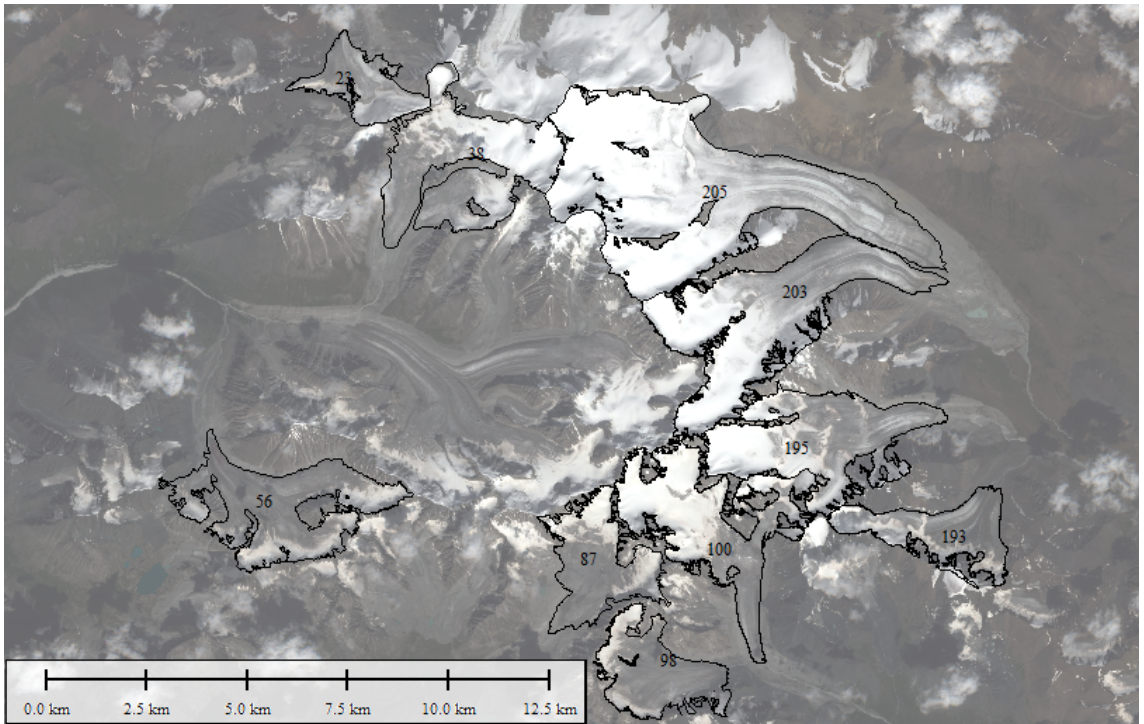
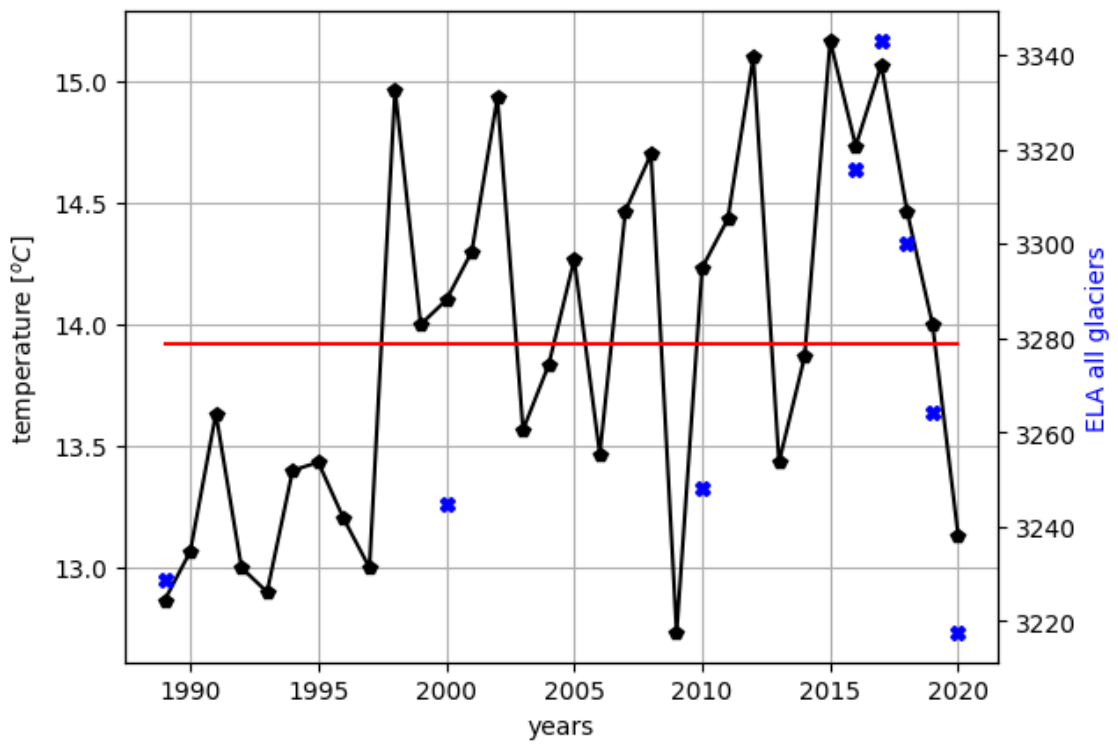


Figure 5: The contours of the examined glaciers with their numbers. The satellite picture was taken on 30th August 2016 and the contours were made manually for a satellite picture from 2010.

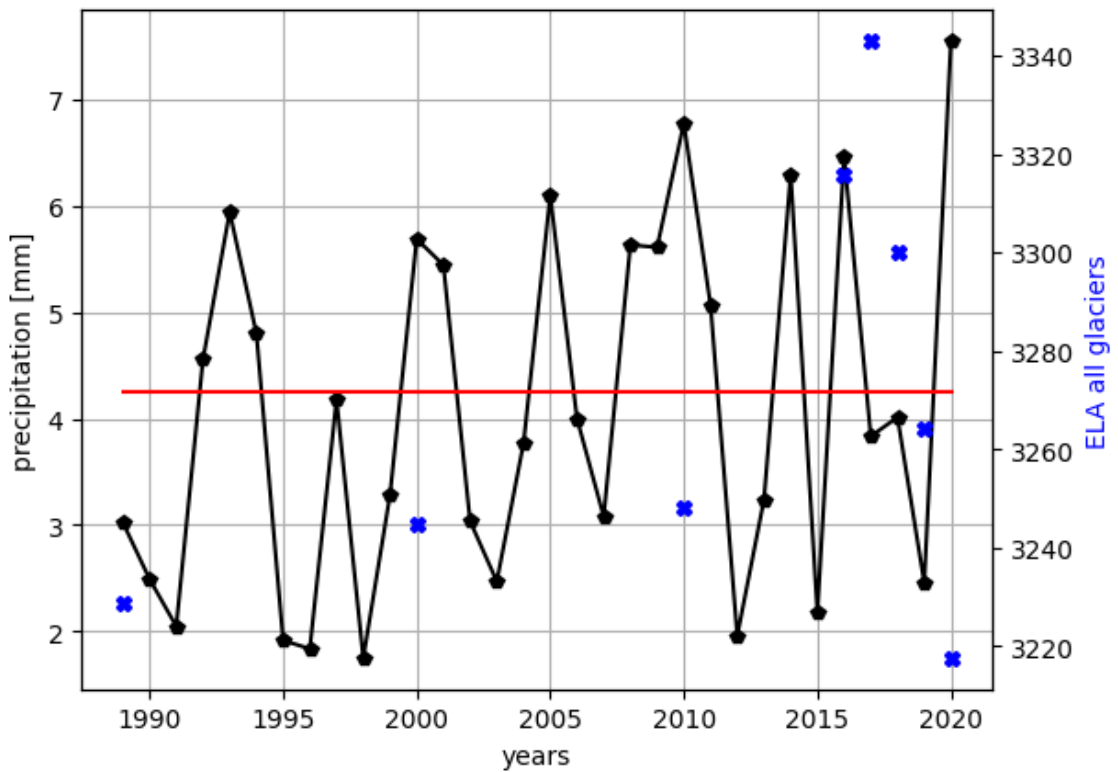
3.1 Temperature and precipitation

In the first step, I processed the data from the Kosh-Agach meteorological station (2.2.). I used the average of the summer temperatures between 1989 and 2020, then plotted them in Figure 4. I also plotted

the average annual precipitation to see the tendencies of the climate variables in the past three decades.



(a) Mean summer temperature (black linked dots) and the average of the ELAs of 10 glaciers in the years 1989, 2000, 2010, 2016, 2017, 2018, 2019, 2020 (blue crosses). The red line is the average of the mean summer temperatures for the whole period. Positive correlation is clearly seen between the temperature and the ELA.



(b) The average precipitation from the previous September until the end of May (black linked dots) and the average of the ELAs of 10 glaciers in the years 1989, 2000, 2010, 2016, 2017, 2018, 2019, 2020 (blue crosses). The red line is the average of the precipitation of the months above for the whole period. Correlation is not seen between precipitation and ELA.

Figure 6: In Figure 6a. temperature and ELA shows strong correlation, while in Figure 6b. correlation is not seen between the precipitation and the ELA.

3.2 Equilibrium line altitude

The equilibrium line altitude were calculated for the above glaciers (Figure 5.). The results of the ELAs are seen in Table 2. In the last row, there are the mean of the ELAs for all the glaciers.

I supplemented the calculated years with the ELAs from the years 2000, 2010, 2020[24] and compared this result with the change of temperature and precipitation. In Table 3., the supplementation of ELAs are seen.

No. \ Year	1989	2016	2017	2018	2019
23	3109	3226	3229	3210	3171
38	3265	3376	3426	3398	3343
56	3122	3247	3258	3225	3182
87	3189	3258	3283	3231	3214
98	3125	3248	3283	3217	3199
100	3206	3302	3361	3280	3268
193	3155	3188	3196	3179	3166
195	3286	3351	3375	3347	3288
203	3366	3381	3424	3370	3360
205	3466	3583	3596	3544	3454
mean	3229	3316	3343	3300	3264

Table 2: The calculated equilibrium line altitudes of the examined glaciers in *meters*. The last row shows the mean ELA for all the measured glaciers.

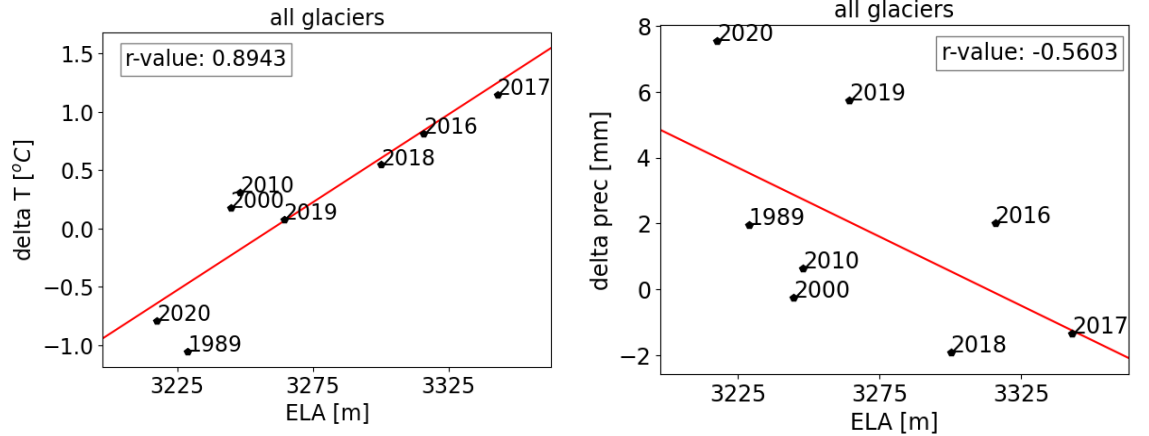
I plotted the calculated ELAs next to the temperature and precipitation data, seen in Figure 6. In Figure 6a., the linked black dots mark the average summer temperature. The horizontal red line is the mean of the summer data in the studied period. Blue dots mark the calculated ELAs in this interval.

Then, I took the average precipitation of the months from previous autumn until the end of the current spring (September, October, November, December, January, February, March, April, May), when the snowfalls and accumulation can happen, for every years between 1989 and 2020. In Figure 6b., the averages of these months are shown

No. \ Year	2000	2010	2020
23	3125	3110	3090
38	3307	3335	3310
56	3150	3130	3110
87	3220	3145	3155
98	3140	3130	3110
100	3280	3250	3225
193	3150	3160	3150
195	3320	3340	3275
203	3326	3380	3340
205	3428	3500	3410
mean	3245	3248	3218

Table 3: The used equilibrium line altitudes of the examined glaciers in *meters*[24]. The last row shows the mean ELA for all the glaciers

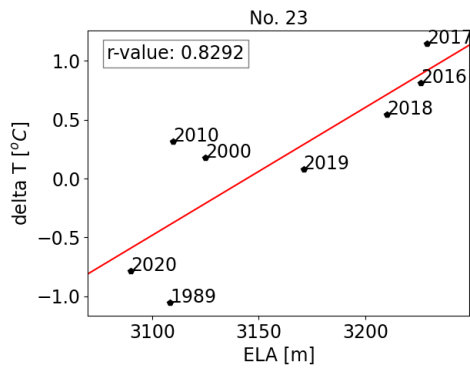
as a function of the years. With the help of these two figures (Figure 6.) we can get a general picture about the climate conditions and the position of ELA.



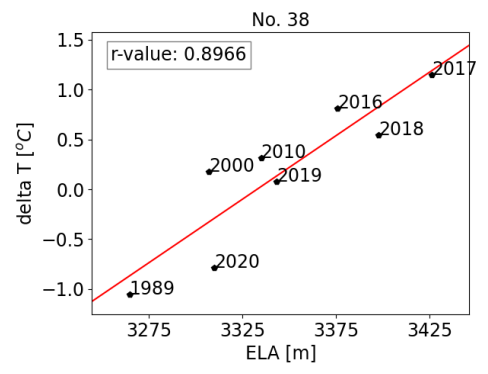
(a) Correlation of the ELA and the difference of the average summer temperature from the mean summer temperature for the whole examined period.

(b) Correlation of the ELA and the difference of the average annual precipitation from the mean annual precipitation for the whole period.

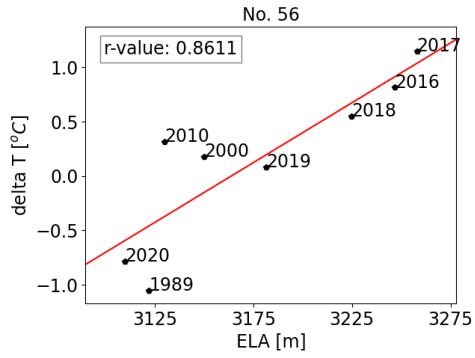
Figure 7: Correlation of the ELAs for the years 1989, 2000, 2010, 2016, 2017, 2018, 2019, 2020. The correlation coefficient is seen in the figures. Between the temperature and ELA, a high correlation is observable, while between the precipitation and the ELA, correlation is not seen.



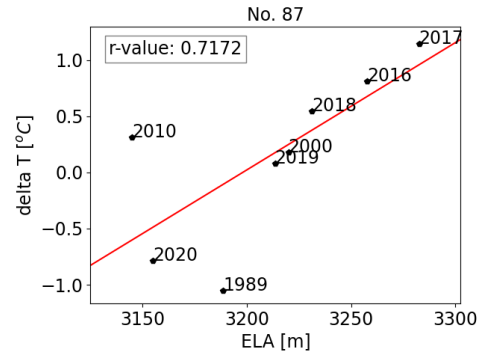
(a)



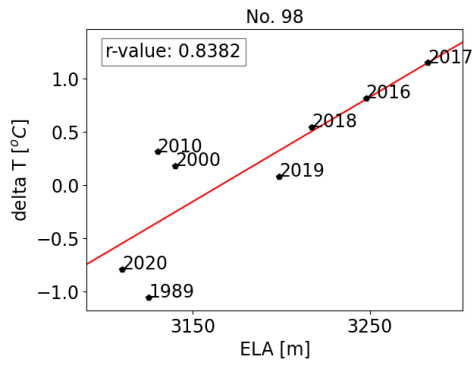
(b)



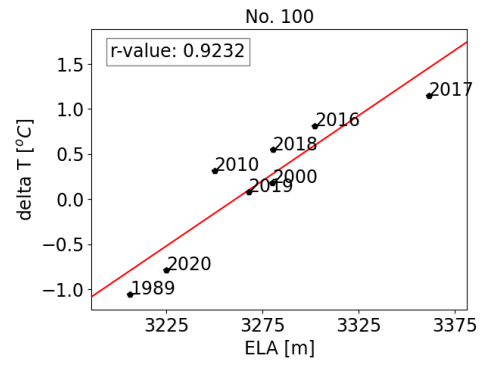
(c)



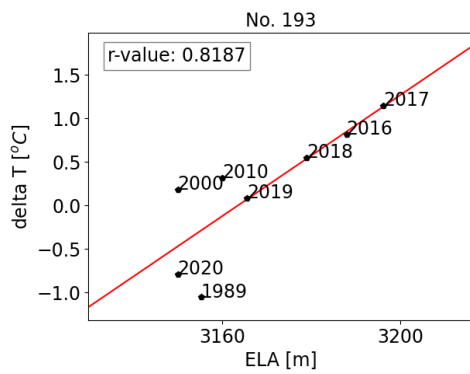
(d)



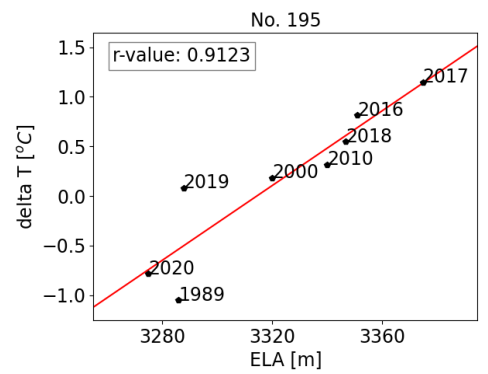
(e)



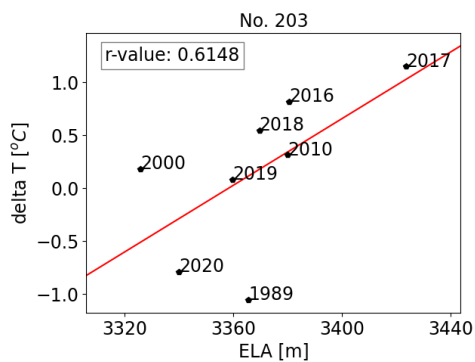
(f)



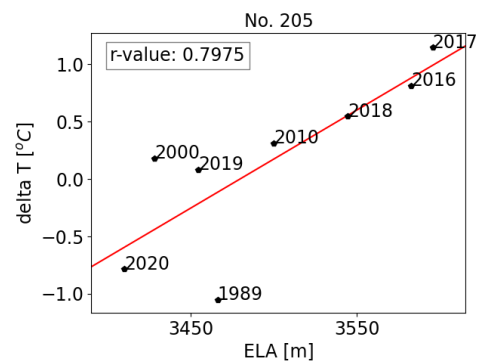
(g)



(h)



(i)



(j)

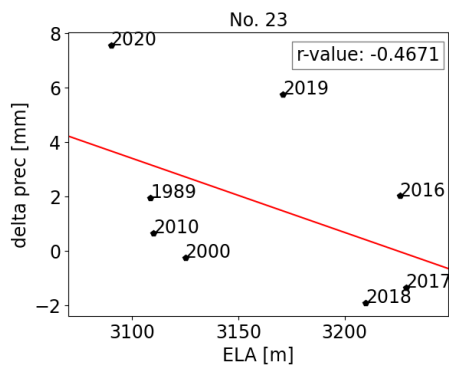
Figure 8: Correlation of the ELA and the temperature for the studied 10 glaciers.

In the next step, I calculated the deviation of the average summer temperature from the mean temperature of the whole period and also the average annual precipitation from the mean precipitation of the whole period. I plotted the deviations of these variables as a function of the ELA. The results are in Figure 7. In the left picture (Figure 7a.), the correlation between the temperature deviation and ELA is plotted, while in the right picture (Figure 7b.), on the vertical axis, the precipitation deviation is seen.

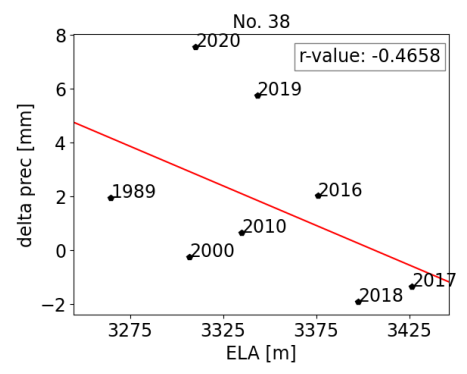
The Pearson's correlation coefficients are also plotted in the figures. There are high positive correlation (r-value= 0.8943) observable between the ELA and temperature, but low negative correlation (r-value= -0.5603) are seen between the ELA and precipitation, which anticipates that the main leading factor of the changes in the ELA is temperature.

This work was done for all the studied 10 glaciers separately, as well. The correlation between the ELAs and temperatures are seen for each glaciers in Figure 8. Most of them show really high correlation (with a Pearson's r-value above 0.8).

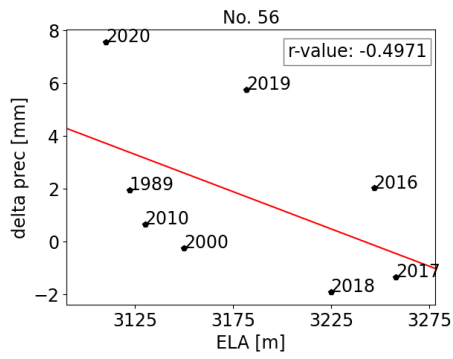
The correlation between the annual precipitation deviation and the ELA for each glaciers is seen in Figure 9. The correlation coefficients show that none of the glaciers depends on the changes of precipitation, hence the changes of precipitation is not a factor can be taken in account when predicting the future behavior of a glacier in the Tavan-Bogd massif.



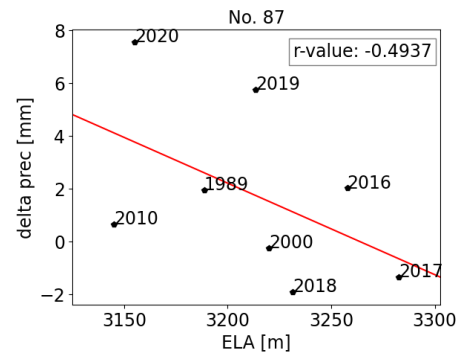
(a)



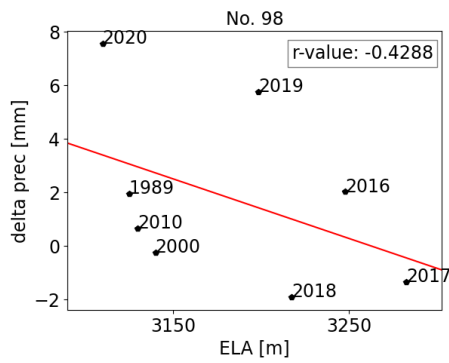
(b)



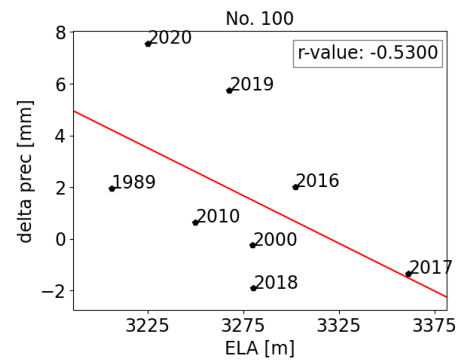
(c)



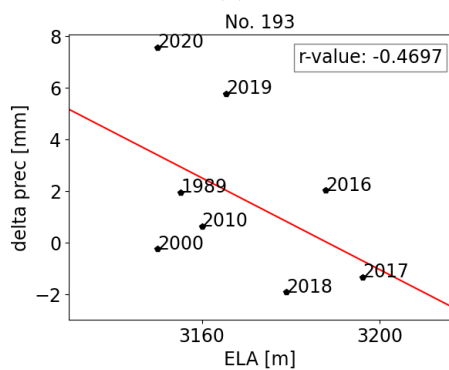
(d)



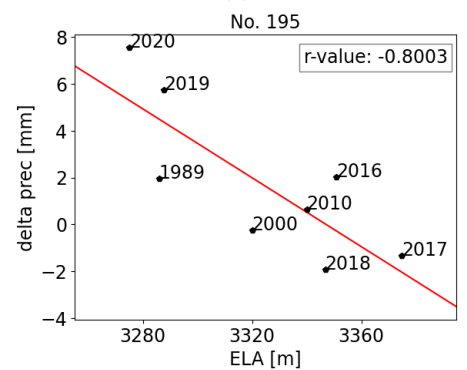
(e)



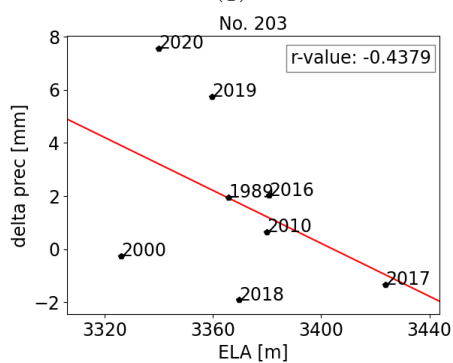
(f)



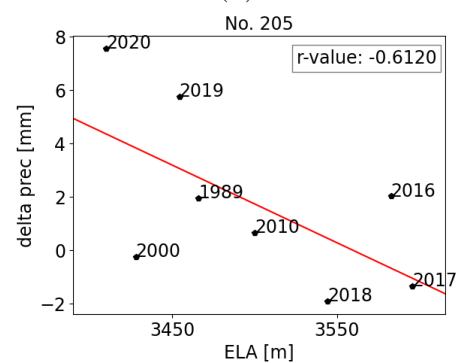
(g)



(h)



(i)



(j)

Figure 9: Correlation of the ELA and the precipitation for the studied 10 glaciers.

3.3 Accumulation area ratio

After calculating the ELAs, the accumulation area ratios were also calculated, for the 10 glaciers above. The calculated AARs are seen in Table 4. Supplementation was also made with the years 2000, 2010, 2020, seen in Table 4. As Figure 10. shows, the accumulation area ratio is also closely following the changes of the temperature.

No. \ Year	1989	2000	2010	2016	2017	2018	2019	2020
23	0.7562	0.5798	0.7442	0.4301	0.4039	0.4855	0.5353	0.5996
38	0.7493	0.6423	0.6661	0.5552	0.4902	0.5714	0.6647	0.7201
56	0.6157	0.5342	0.5932	0.3463	0.2907	0.4357	0.5197	0.6704
87	0.5895	0.4593	0.7076	0.4223	0.3652	0.5047	0.5381	0.6514
98	0.4788	0.5034	0.5432	0.2335	0.1588	0.2681	0.3230	0.5228
100	0.7879	0.6586	0.7387	0.6945	0.6453	0.6998	0.7236	0.7712
193	0.5426	0.5607	0.5585	0.4861	0.4407	0.5133	0.5072	0.6011
195	0.6063	0.5312	0.5920	0.4390	0.4779	0.5477	0.6062	0.6445
203	0.6456	0.6692	0.6363	0.5762	0.4657	0.5906	0.6380	0.6687
205	0.6534	0.6766	0.6277	0.5353	0.4896	0.5717	0.6559	0.7007
mean	0.6425	0.5815	0.6407	0.4719	0.4228	0.5189	0.5712	0.6551

Table 4: The AARs of the examined glaciers calculated from the ELAs in 3.2.

In Figure 11., the correlation between the average summer temperature (left) and average annual precipitation (right) is seen. As it was for the case of ELA, the correlation of AAR is high for the temperature and low for the precipitation. It confirms the assumption that, following the trends of the summer temperature, the future changes of the glaciers is predictable.

Figure 12. shows the correlation between the temperature and AAR for each glaciers, separately. High negative correlation is seen for every studied glaciers, what means that the AARs show strong relation with the temperature, similar to the ELAs. The lowest r-value is -0.6632 for the glacier No. 87 and highest is -0.9492 for glacier No. 38.

However, annual precipitation shows low correlation with the AARs for almost all the glaciers, generally. The highest r-value 0.6178 for

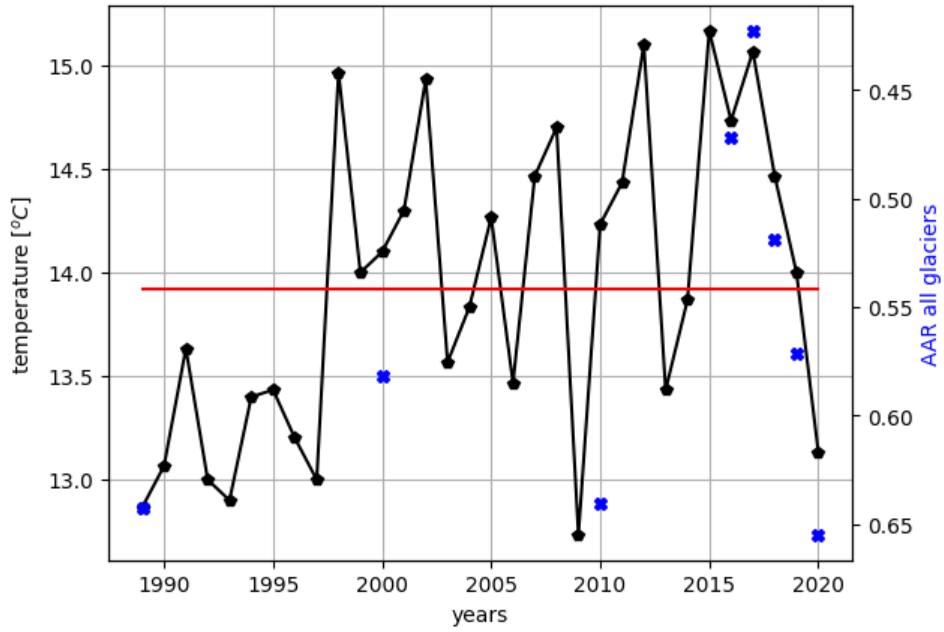
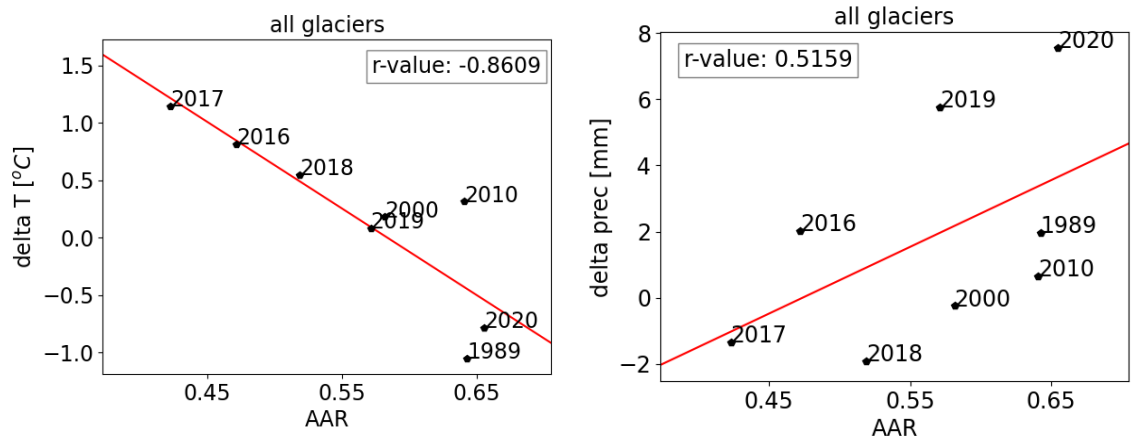


Figure 10: Mean summer temperature (black linked dots) and the average of the AARs of 10 glaciers in the years 1989, 2000, 2010, 2016, 2017, 2018, 2019, 2020 (blue crosses). The red line is the average of the mean summer temperatures for the whole period. Positive correlation is clearly seen between the temperature and the AAR, similar to the behavior of the temperature and the ELA (Figure 6a).

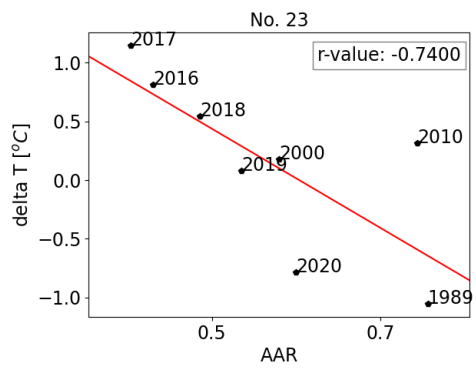
glacier No. 100, therefore, we can state that precipitation cannot be used for forecasting.



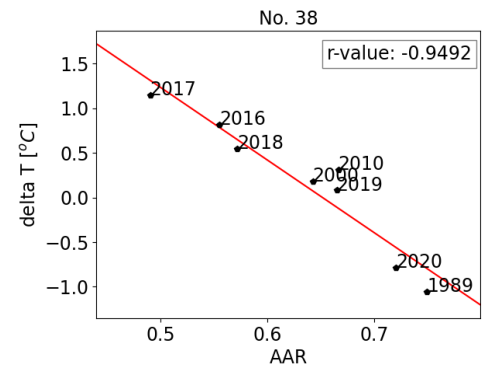
(a) Correlation of the AAR and the difference of the average summer temperature from the mean summer temperature for the whole examined period.

(b) Correlation of the AAR and the difference of the average annual precipitation from the mean annual precipitation for the whole period.

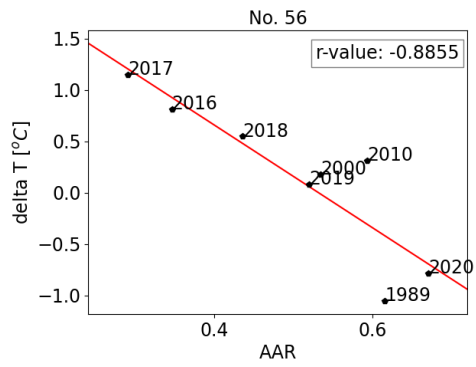
Figure 11: Correlation of the AARs for the years 1989, 2000, 2010, 2016, 2017, 2018, 2019, 2020. The correlation coefficient is seen in the figures. Between the temperature and AAR, a high correlation is observable, while between the precipitation and the AAR, correlation is not seen. The results are similar to the results in Figure 7



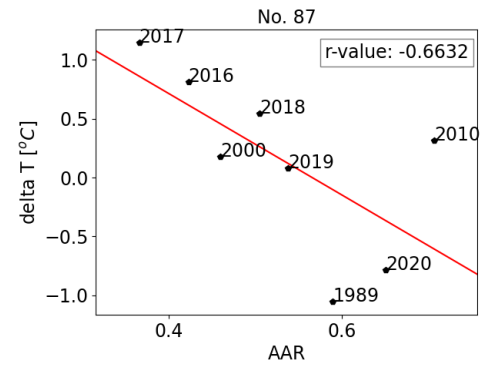
(a)



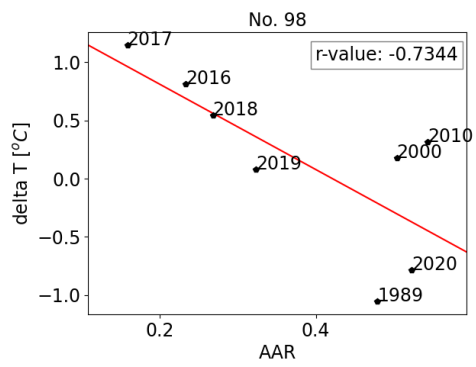
(b)



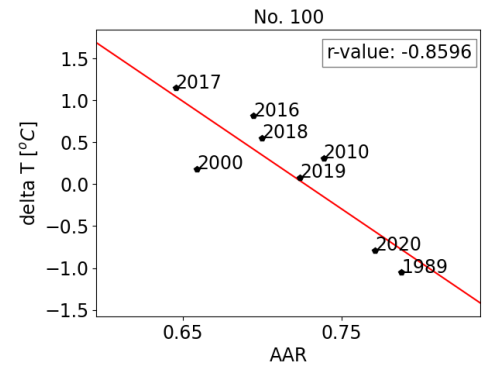
(c)



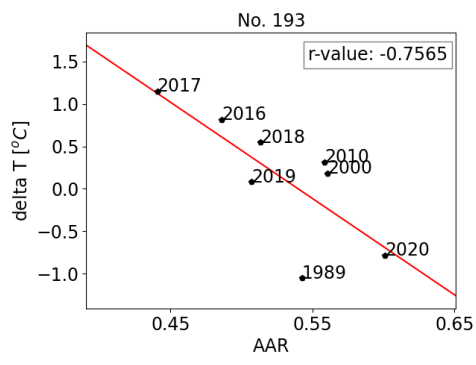
(d)



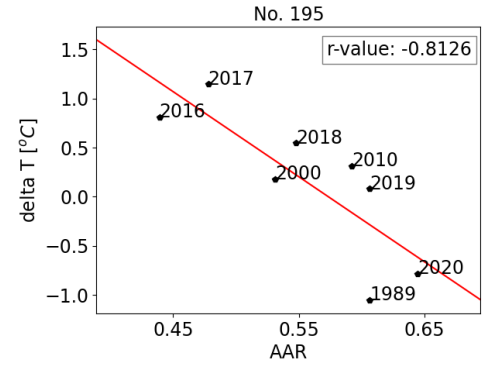
(e)



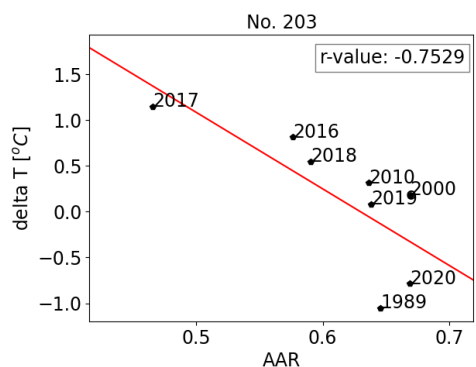
(f)



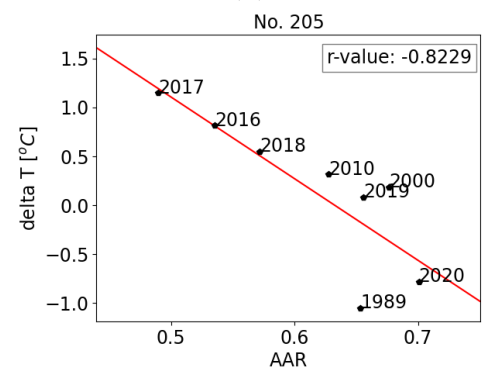
(g)



(h)

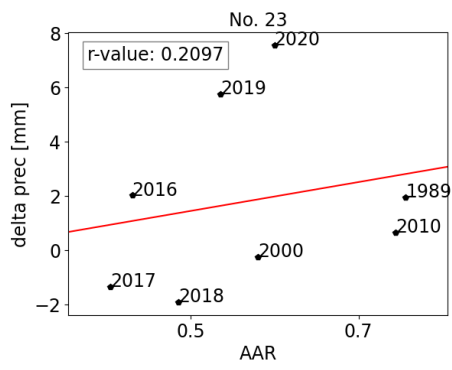


(i)

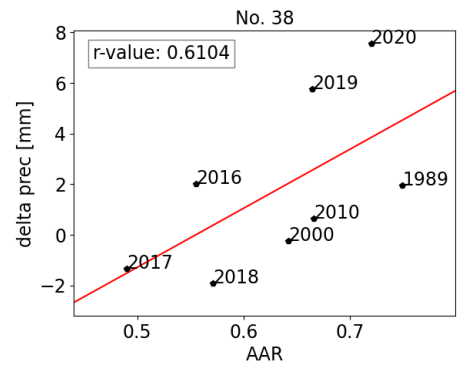


(j)

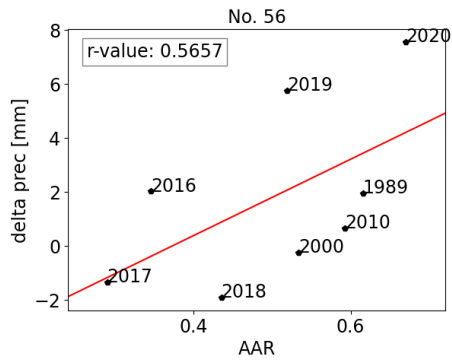
Figure 12: Correlation of the AAR and the temperature for the studied 10 glaciers.



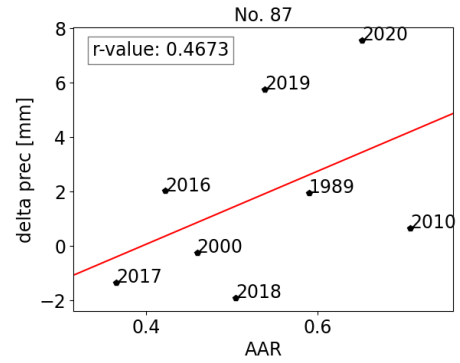
(a)



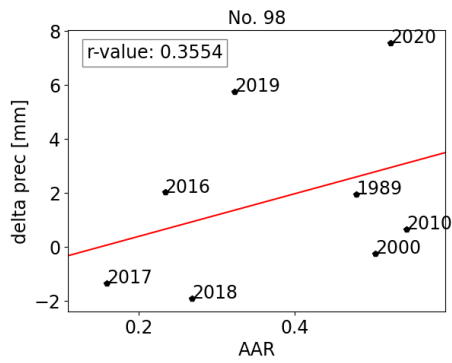
(b)



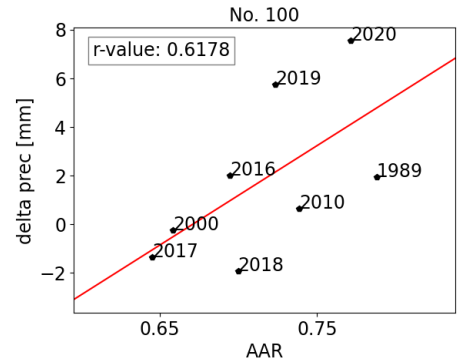
(c)



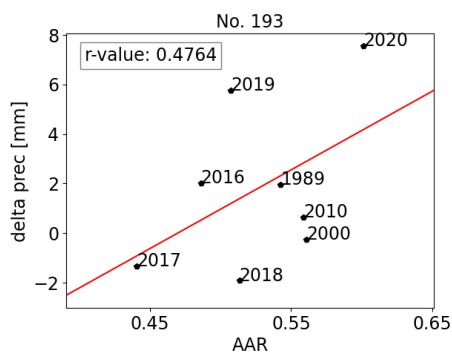
(d)



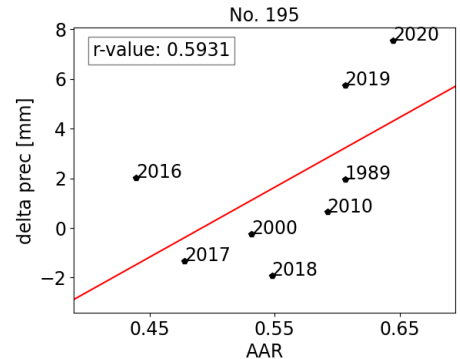
(e)



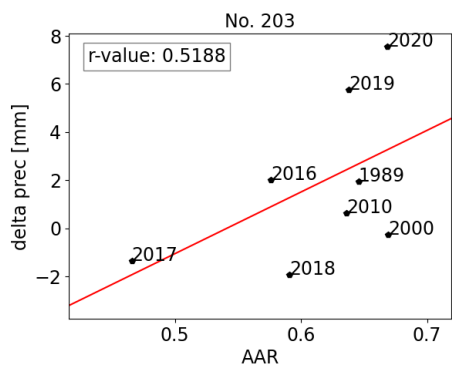
(f)



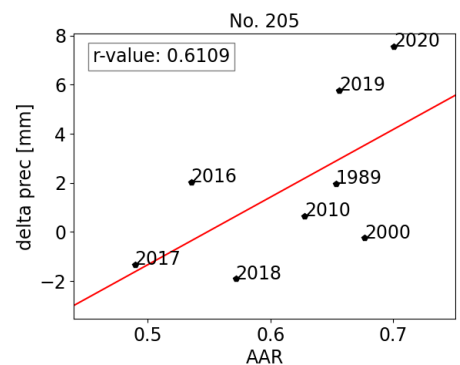
(g)



(h)



(i)



(j)

Figure 13: Correlation of the AAR and the precipitation for the studied 10 glaciers.

4 Discussion

4.1 Tendencies in the temperature and precipitation

In the Altai mountain region, a general increasing tendency of temperature was observed during the examined past three decades from 1989 to 2020. The data from Kosh-Agach meteorological station is supported by temperature trends measured in the surrounding meteorological stations (Kara-Tyurek 2600*m*, Akkem 2050, Akturu 2025*m*). A general increase in precipitation was also observable in these weather stations. In contrast, in the meteorological station Kosh-Agach 1759*m*, Bertek 2250*m* and Mugur-Aksy 1830*m*, this increase in precipitation is not so obvious[27].

However, based on the Kosh-Agach data, in the last three years, a constant decrease is seen and the temperature in 2020, approaches the temperature in 1989 (Figure 4.). In addition, in 2009, a significant drop in temperature is visible. In the meantime, the precipitation shows increasing tendency and that can be an explanation for the temperature drop, because the increased precipitation usually results lower temperature. It results that, generally, between the precipitation and temperature, an inverse relationship is observable. Thus, usually warmer summers mean less precipitation.

Unfortunately, without knowing the data for the following years, it is hard to tell whether this behavior is a trend or just outstanding values. For example, in the year 2009, it is clearly seen that the temperature had an outlier value, but regarding the last three years, it is hard to predict the following year.

Looking the temperature and the precipitation together in Figure 4., we can distinguish periods, which was not favorable for glacial growth. These periods are characterized by high temperatures and low precipitation. For example, between 1997 and 2006, the climate conditions were extremely bad for glaciers. It is also true for the periods from 2014 to 2018, which resulted the high position of the ELA as we can see in

Table 2. for the years 2016, 2017 and 2018. Nevertheless, because of the lack of data, we could only assume that the ELA was in a high position between 2014 and 2018, as well.

4.2 Forecasting the glacial behavior

In the previous section, it was found that the temperature plays huge role in glacial behavior of the examined 10 glaciers (Figure 5.). On the contrary, precipitation does not show strong connection and clear correlation with glacial dynamics. It results that if we want to do predictions, we should only consider one factor, the temperature, instead of two factors, both the temperature and the precipitation.

In the past three decades, the average tendency of all the glacier shows that, 1 degree of Celsius results 66.5 meters change in the equilibrium line altitude. In other words, the position of the equilibrium line will change with 100m, if the temperature changes $1.5^{\circ}C$.

With this general trend of the valley glaciers in the Tavan Bogd massif and knowing the exact gradient of the equilibrium line altitude, it becomes possible to give predictions for the future behavior of these larger glaciers. Especially, since these glaciers are not that much exposed to the rapid changes in temperature and precipitation or individual morphological properties, like the smaller ones (for example hanging or cirque glaciers).

Examining the correlation between the changes in the equilibrium line altitudes of the glaciers in the region and the changes in temperature at Kosh-Agach meteorological station more closely, we can get a broader view of what factors may still influence the change of the ELA.

On one hand, a positive correlation is clearly seen in Figure 7a., but on the other hand, in Figure 7b., it shows very low correlation. This small correlation is seen, despite the fact that, former climate analyzes[27] have shown that the precipitation data from Kosh-Agach weather station has less correlation with the precipitation data from

Bertek weather station (which was the closest station in the past). However, precipitation can also have a huge impact on the position of the equilibrium line. In Figure 8., looking at the correlation one by one for each glacier, some years, for example, the year 1989, stand out multiple times. Taking a look at the precipitation from the last accumulation period before the summer of 1989, it is seen that the precipitation was really low. (Figure 6b). It causes that, in spite of the low temperature (Figure 6a), there was not enough precipitation (snowfalls) to melt, so the equilibrium line occupied a higher position. In the same way, regarding the years 2000 and 2010, precipitation was relatively high in both years, which moved the equilibrium line to a lower position, than it was expected by only looking at the temperature data.

It was also found that, the accumulation area ratio also stands in a strong relation with the temperature. The negative correlation is seen in Figure 10. Moreover, Table 4. shows the annual changes of the AARs, separately, for each examined glacier. The typical AAR values can be seen both for the better and the worse climate conditions, from the view of the glacial accumulation. In this study, the minimum value of the AAR is 0.159, which was measured in 2017 for the glacier No. 98. As it is seen in Figure 5., it is one of the smaller glaciers, with a completely eastward orientation. Hence, this glacier is probably more exposed to changes of precipitation and to its own morphological structure (slope angle, altitude). Besides that, the maximum measured AAR was 0.771 in the year 2020 for the glacier No. 100. This glacier has a very special shape and a southward orientation, which could cause the relatively high AAR values for every year. Examining the extreme values of the AARs, the amplitude of the AARs was found to be about 0.612.

Basically, the bulk of the AARs vary between 0.30 and 0.70 with an average $AAR_{avg} = 0.563$. Hence, it can be said that, when the climate conditions are better for the glaciers, the AAR will be higher than this average AAR_{avg} value and when conditions are bad for glacial growth, the AAR of the glaciers will be lower than the average AAR_{avg} . Dyurgurov et al.[37] developed a new index for monitoring glacial change and

measuring the delay in their dynamic response using the time-averaged $\langle \text{AAR} \rangle$ and the equilibrium state AAR_0 . According to their result, the average equilibrium state AAR_0 remains the same over the time and does not change with the climate. In this article, this AAR_0 value was determined at 0.579 ± 0.009 for tropical glaciers, which approaches the value I got for glaciers in the Tavan Bogd massif.

The AARs can be also calculated with the Kurowski method (2.3). Ganyushkin et al. [24] made a comparison between the measured AARs and calculated AARs based on the Kurowski method for the years 1989, 2000, 2010 and 2020. They found that the difference between the AAR calculated with the Kurowski method and the measured AAR from the satellite pictures is only -0.12 . However, it should be considered that the satellite pictures could not be taken exactly at the equilibrium state (because it is not always available), therefore they are only close approximations of the balanced-budget state, so the real position of ELA can be even closer to the ELAs calculated by Kurowski method. That means Kurowski method can be used with a good approximation for calculating the ELAs and AARs and with a large number of glaciers, using it can be very beneficial and can facilitate the work, because of its ease of use, in contrast the method above.

Since the equilibrium line altitude follows the changes of temperature, we can use it to predict the glacial termini. Assuming that the AAR remains the same over the time, we can use the average value of the accumulation area ratio ($\text{AAR}_{avg} = 0.563$). After calculating the future position of the ELA using the gradient above ($66.5 \frac{m}{^\circ C}$), the ablation area can be adjusted so we can have a prediction for the area of a glacier and even the terminus of a glacier can be estimated. So we developed a method to predict the typical glacial behavior in the examined area.

5 Conclusion

In this work, 10 larger glaciers in the Tavan Bogd massif were examined, mostly on the eastern part of the massif. First, climate conditions (temperature and precipitation) using the data from Kosh-Agach meteorological station were examined to get an overview about the leading trend in the past three decades, from 1989 to 2020.

Then, satellite pictures from United States Geological Survey (USGS) were obtained. Analysis were made for four consecutive years (from 2016 to 2019) and the year 1989 with different Geographic Information Systems to determined the equilibrium line altitudes (ELA) of the examined glaciers. Calculation of the accumulation area ratio (AAR) was also done for each glacier. The data series was expanded with previous calculations[24] with the results of the years 2000, 2010 and 2020.

A strong correlation was observed between the temperature and ELA, with a correlation coefficient 0.8943 between the average ELA of the 10 glaciers and the average summer temperature. However, it was found that between the precipitation and the ELA, there is no strong relation. It means that only one factor, the calculated gradient of the equilibrium line altitude ($66.5 \frac{m}{^{\circ}C}$), can be used for predicting the future position of the ELA in the Tavan Bogd massif.

Using the time average value of the calculated AARs ($AAR_{avg} = 0.563$), it became possible to predict other properties of the glaciers, as well, such as glacial termini or the total area of the glaciers.

Although it was used only 8 data points, the correlation proved to be strong, but if we studied more years we could get a more accurate relation about the trends, which is one of the goals for the future. An other further work is to calculate the mass balance for the glaciers above. In addition, it would be interesting to compare the results with the Kurowski method for each years using the mass balance of the glaciers. Unfortunately, this method cannot tell, how inert is a glacier for the change of the temperature, it requires further researches.

Finally, after using this method to predict the future behavior of the glaciers, in situ measurements can give an interesting comparison and can be used to verify and to improve the accuracy of this model.

Acknowledgements

In the first place, I would like to acknowledge my supervisor, Prof. Dr. Dmitry A. Ganyushkin, who helped me through this project. I would like to thank him the interesting topic recommendation and the great amount of help he gave me during the research. I really appreciate his flexibility and his patience, despite of the difficult external conditions that made the work mostly remote.

I would also like to thank my family who was always beside me to help me solving the problems I faced during my studies. I need to highlight my boyfriend for the encouragement he gave me while I was writing my thesis. I cannot finish without mentioning my classmates, who became my friends throughout the years and provided me infinite amount of help during my studies.

Finally, I am thankful for the Saint Petersburg State University and also Hamburg University that made my master studies possible.

References

- [1] P. U. Clark, A. S. Dyke, J. D. Shakun, *et al.*, “The last glacial maximum,” *Science*, vol. 325, no. 5941, pp. 710–714, 2009. DOI: 10.1126/science.1172873. eprint: <https://www.science.org/doi/pdf/10.1126/science.1172873>. [Online]. Available: <https://www.science.org/doi/abs/10.1126/science.1172873>.
- [2] R. G. Fairbanks, “A 17,000-year glacio-eustatic sea level record: Influence of glacial melting rates on the younger dryas event and deep-ocean circulation,” *Nature*, vol. 342, no. 6250, pp. 637–642, Dec. 1989, ISSN: 1476-4687. DOI: 10.1038/342637a0. [Online]. Available: <https://doi.org/10.1038/342637a0>.
- [3] M. F. Meier, *Glacier*. Encyclopædia Britannica, inc., Mar. 2022. [Online]. Available: <https://www.britannica.com/science/glacier>.
- [4] K. Cuffey and W. Paterson, *The Physics of Glaciers. 4th edition*. 2010.
- [5] J. Oerlemans, “Quantifying global warming from the retreat of glaciers,” *Science*, vol. 264, no. 5156, pp. 243–245, 1994. DOI: 10.1126/science.264.5156.243. eprint: <https://www.science.org/doi/pdf/10.1126/science.264.5156.243>. [Online]. Available: <https://www.science.org/doi/abs/10.1126/science.264.5156.243>.
- [6] M. F. Meier, M. B. Dyurgerov, U. K. Rick, *et al.*, “Glaciers dominate eustatic sea-level rise in the 21st century,” *Science*, vol. 317, no. 5841, pp. 1064–1067, Aug. 2007.
- [7] D. Ganyushkin, K. Chistyakov, I. Volkov, *et al.*, “Present glaciers of tavan bogd massif in the altai mountains, central asia, and their changes since the little ice age,” *Geosciences (Switzerland)*, vol. 8, pp. 1–35, Nov. 2018. DOI: 10.3390/geosciences8110414.
- [8] D. Ganyushkin, K. Chistyakov, I. Volkov, D. Bantcev, E. Kunaeva, and N. Kharlamova, “Modern data on glaciation of the northern slope of tavan-bogdo-ola massif (altai) -- () modern data on glaciation of the northern slope of tavan-bogdo-ola massif (altai),” *Ice and Snow*, vol. 57, pp. 307–325, Oct. 2017. DOI: 10.15356/2076-6734-2017-3-307-325.
- [9] D. Ganiushkin, K. Chistyakov, and E. Kunaeva, “Fluctuation of glaciers in the southeast russian altai and northwest mongolia mountains since the little ice age maximum,” *Environmental Earth Sciences*, vol. 74, pp. 1883–1904, 2015.

- [10] V. Sapozhnikov, *Mongolian altai in the sources of the irtysh and kobdo. travels of 1906–1911*, 1911.
- [11] B. Tronov, “Catalog of altai glaciers,” *Bull. Russ. Geogr. Soc*, vol. 57, pp. 107–159, 1925.
- [12] W. Lilun, L. Chaohai, and W. Ping, “Modern glaciers in altai mountains of china,” *Acta Geogr. Sin*, vol. 40, pp. 142–153, 1985.
- [13] “The ussr glacier inventory,” *Katalog lednikov SSSR*, vol. 15, p. 47, 1977.
- [14] Z. Bjamba and E. Selivanov, “Present glaciation of mongolia,” *Bull. All-Union Geogr. Soc*, vol. 103, pp. 249–254, 1971.
- [15] V. Revyakin and R. Mukhametov, “Dynamics of the glaciers of the tabynbogdo-ola,” *Glaciology of Siberia*, vol. 4, no. 19, pp. 83–92, 1993.
- [16] U. KAMP and C. G. PAN, “Inventory of glaciers in mongolia, derived from lands at imagery from 1989 to 2011,” *Geografiska Annaler. Series A, Physical Geography*, vol. 97, no. 4, pp. 653–669, 2015, ISSN: 04353676, 14680459. [Online]. Available: <http://www.jstor.org/stable/43870874> (visited on 05/19/2022).
- [17] W. Guo, S. Liu, J. Xu, *et al.*, “The second chinese glacier inventory: Data, methods and results,” *Journal of Glaciology*, vol. 61, no. 226, pp. 357–372, 2015. DOI: 10.3189/2015JoG14J209.
- [18] B. S. Krumwiede, U. Kamp, G. J. Leonard, J. S. Kargel, A. Dashtseren, and M. Walther, “Recent glacier changes in the mongolian altai mountains: Case studies from munkh khairkhan and tavan bogd,” in *Global Land Ice Measurements from Space*, J. S. Kargel, G. J. Leonard, M. P. Bishop, A. Kääb, and B. H. Raup, Eds. Berlin, Heidelberg: Springer Berlin Heidelberg, 2014, pp. 481–508, ISBN: 978-3-540-79818-7. DOI: 10.1007/978-3-540-79818-7_22. [Online]. Available: https://doi.org/10.1007/978-3-540-79818-7_22.
- [19] K. M. Cuffey and W. S. B. Paterson, *The physics of glaciers*. Academic Press, 2010.
- [20] G. Peterson, *Accumulation area ratio and equilibrium line altitude on the southern patagonia icefield, 2000-2010, retrieved using modis satellite images*, 2010.
- [21] F. Müller, “Zonation in the accumulation area of the glaciers of axel heiberg island, nwt, canada,” *Journal of Glaciology*, vol. 4, no. 33, pp. 302–311, 1962.

- [22] M. F. Meier and A. S. Post, *Recent variations in mass net budgets of glaciers in western North America*, English. 1962, crossref: <https://www.coldregions.org/vufind/Record/19973>.
- [23] D. Benn and F. Lehmkuhl, “Mass balance and equilibrium-line altitude of glaciers in high mountain environments,” *Quaternary International*, vol. 65, pp. 15–29, Apr. 2000. DOI: 10.1016/S1040-6182(99)00034-8.
- [24] D. Ganyushkin, K. Chistyakov, E. Derkach, *et al.*, “Glacier recession in the altai mountains after the lia maximum,” *Remote Sensing*, vol. 14, no. 6, 2022, ISSN: 2072-4292. DOI: 10.3390/rs14061508. [Online]. Available: <https://www.mdpi.com/2072-4292/14/6/1508>.
- [25] *Climatic conditions over the territory of russia*, <http://meteo.ru/>, Accessed: 2022-05-20.
- [26] *United states geological survey (usgs)*, <https://earthexplorer.usgs.gov/>, Accessed: 2022-05-19.
- [27] D. A. Ganyushkin, K. V. Chistyakov, I. V. Volkov, D. V. Bantcev, E. P. Kunaeva, and A. V. Terekhov, “Present glaciers and their dynamics in the arid parts of the altai mountains,” *Geosciences*, vol. 7, no. 4, 2017, ISSN: 2076-3263. DOI: 10.3390/geosciences7040117. [Online]. Available: <https://www.mdpi.com/2076-3263/7/4/117>.
- [28] W. McKinney, “Data Structures for Statistical Computing in Python,” in *Proceedings of the 9th Python in Science Conference*, S. van der Walt and J. Millman, Eds., 2010, pp. 56–61. DOI: 10.25080/Majora-92bf1922-00a.
- [29] G. Van Rossum and F. L. Drake, *Python 3 Reference Manual*. Scotts Valley, CA: CreateSpace, 2009, ISBN: 1441412697.
- [30] L. Kurowski, *Die Höhe der Schneegrenze: mit besonderer Berücksichtigung der Finsteraarhorn-Gruppe*. na, 1891.
- [31] R. J. Braithwaite, “From doktor kurowski’s schneegrenze to our modern glacier equilibrium line altitude (ela),” *The Cryosphere*, vol. 9, no. 6, pp. 2135–2148, 2015. DOI: 10.5194/tc-9-2135-2015. [Online]. Available: <https://tc.copernicus.org/articles/9/2135/2015/>.
- [32] H. Osmaston, “Estimates of glacier equilibrium line altitudes by the area \times altitude, the area \times altitude balance ratio and the area \times altitude balance index methods and their validation,” *Quaternary International*, vol. 138-139, pp. 22–31, 2005, Snowlines at the Last Glacial Maximum and tropical cooling, ISSN:

- 1040-6182. DOI: <https://doi.org/10.1016/j.quaint.2005.02.004>. [Online]. Available: <https://www.sciencedirect.com/science/article/pii/S104061820500039X>.
- [33] B. R. Rea, “Defining modern day area-altitude balance ratios (aabrs) and their use in glacier-climate reconstructions,” *Quaternary Science Reviews*, vol. 28, no. 3, pp. 237–248, 2009, Special Theme: Modern Analogues in Quaternary Palaeoglaciological Reconstruction (pp. 181-260), ISSN: 0277-3791. DOI: <https://doi.org/10.1016/j.quascirev.2008.10.011>. [Online]. Available: <https://www.sciencedirect.com/science/article/pii/S0277379108002989>.
- [34] C. E. S. R. I. Redlands, *Arcgis desktop: Release 10*, 2011.
- [35] *Earth resources observation and science (eros) center*, <https://www.usgs.gov/centers/eros>, Accessed: 2022-05-21.
- [36] L. Daniel, *Inside MapInfo professional : the friendly user guide to MapInfo professional*, eng, 3rd ed. Australia ; OnWord Press, 2002, ISBN: 0766834727.
- [37] M. Dyurgerov, M. F. Meier, and D. B. Bahr, “A new index of glacier area change: A tool for glacier monitoring,” *Journal of Glaciology*, vol. 55, no. 192, pp. 710–716, 2009.